Published in final edited form as:
Mol Pharm. 2013 July 1; 10(7): 2558–2567. doi:10.1021/mp300702x.

Single-Antibody, Targeted Nanoparticle Delivery of Camptothecin

Han Han and **Mark E. Davis***
Chemical Engineering, California Institute of Technology, Pasadena, CA 91125

Abstract

We have developed a new method for assembling targeted nanoparticles that utilizes the complexation between targeting agents that contain boronic acids and polymer-drug conjugates that possess diols. Here, we report the first *in vivo*, antitumor results of a nanoparticle formed via this new assembly methodology. A nanoparticle consisting of a mucic acid polymer conjugate of camptothecin (CPT), MAP-CPT; and containing on average one Herceptin antibody is investigated in nude mice bearing HER2 overexpressing BT-474 human breast cancer tumors. Nontargeted MAP-CPT and antibody-containing MAP-CPT nanoparticles of ca. 30–40 nm diameter and slightly negative zeta potential show prolonged *in vivo* circulation and similar biodistributions after intravenous tail vein injections in mice. The maximum tolerated dose (MTD) of the nontargeted and Herceptin-containing MAP-CPT nanoparticles are found to be 10 and 8 mg CPT/kg, respectively, in mice. Mice bearing BT-474 human breast tumors treated with nontargeted MAP-CPT nanoparticles at 8 mg CPT/kg show significant tumor growth inhibition (mean tumor volume of 63 mm^3) when compared to Irinotecan at 80 mg/kg (mean tumor volume of 575 mm^3) and CPT at 8 mg/kg (mean tumor volume of 808 mm^3) at the end of the study. Herceptin antibody treatment at 5.9 mg/kg results in complete tumor regressions in 5 out of 8 mice, with a mean tumor volume of 60 mm^3 at the end of the study. Mice treated with MAP-CPT nanoparticles at 1 mg CPT/kg do not show tumor inhibition. However, all mice receiving administrations of MAP-CPT nanoparticles (1 mg CPT/kg) that contain on average a single Herceptin molecule per nanoparticle (5.9 mg Herceptin equivalent/kg) show complete tumor regression by the end of the study. These results demonstrate that the antitumor efficacy of nanoparticles carrying anticancer drugs can be enhanced by incorporating on average a single antibody.

Keywords

Targeted nanoparticles; Herceptin; camptothecin; antitumor efficacy; biodistribution

Introduction

Campthothecin (CPT) is a highly potent, naturally occurring anticancer alkaloid that acts by inhibiting both topoisomerase I and HIF-1α activities.[1,2] However, its systemic delivery is problematic due to its low aqueous solubility and nonspecific toxicity. Under aqueous conditions, CPT exists as either an active lactone form, that has anticancer properties, or as an inactive carboxylate form, that has higher toxicity.[3,4] The carboxylate form of CPT is favored at physiological pH, and serum albumin preferentially binds to the carboxylate form resulting in an equilibrium shift towards further CPT deactivation.[5] The FDA approved CPT derivatives Irinotecan (Camptostar™) and Topotecan (HycamptinTM) are used to treat solid

*To whom correspondence should be addressed, mdavis@cheme.caltech.edu.

tumors in a variety of cancers. However, the low percentages of the active form in circulation, drug resistance and toxicity issues limit their clinical efficacy and applications.[6–9]

A variety of polymers conjugated with CPT have been and are currently being evaluated in clinical trials for the treatment of solid tumors.[10–13] These molecular conjugates and nanoparticles exploit the enhanced permeability and retention (EPR) effect that results in the preferential accumulation of macromolecules in solid tumors.[14] To increase cancer cell uptake of nanoparticles that have reached the tumor site by the EPR effect, targeting ligands against overexpressed or specific receptors on cancer cell surfaces can be placed on the surfaces of the nanoparticles. These targeted nanoparticles are taken into tumor cells via receptor-mediated endocytosis. Studies show that the targeted nanoparticles demonstrate higher cellular uptake compared to their nontargeted nanoparticle counterparts with similar sizes and surface charges.[15–17]

Antibody therapy has received wide attention due to its ability to selectively target tumor cells through receptor-specific interactions.[18] However, antibody therapy can rarely achieve complete remissions, neither as a single agent, nor when used in combination with chemotherapy.[19,20] An example is Herceptin. (Trastuzumab), an antibody against HER2 (human epidermal growth hormone receptor 2) tyrosine kinase that is overexpressed in 20% to 30% of breast cancers and is associated with resistance to therapy and a poor prognosis.[21,22] Herceptin is used in the clinic as a single agent after adjuvant chemotherapy, or in combination with chemotherapy to treat HER2 overexpressing metastatic breast cancers.[23,24] Treatments containing Herceptin show better response compared to chemotherapy alone. However, a significant proportion of patients treated in this manner either do not respond or relapse after a period of clinical response.[23,25,26]

To improve the antitumor efficacy of antibody therapy, the selective tumor targeting capability of an antibody can be combined with the cytotoxic ability of an anticancer drug by the coupling of these two therapeutics to form an antibody-drug conjugate.[27,28] The antibody-drug conjugate brentuximab vedotin (Adcetris®) has been FDA approved to treat Hodgkin's lymphoma and anaplastic large-cell lymphoma expressing the antigen CD30.[29] It is composed of an antibody specific for CD30 conjugated with approximately four molecules of the antimicrotubule drug monomethyl auristatin E (MMAE).[30] Treatment with brentuximab vedotin alone in relapsed or refractory Hodgkin lymphoma patients resulted in a complete response rate of 34%; in relapsed or refractory systemic anaplastic large-cell lymphoma patients, it gave a complete remission rate of 57%.[31,32] The recently FDA approved antibody-drug conjugate, trastuzumab emtansine (Kadcyla®), is used for the treatment of metastatic breast cancers and is comprised of a Herceptin antibody conjugated with approximately three molecules of the cytotoxic emtansine.[33] Patients with HER2 overexpressing metastatic breast cancers treated with trastuzumab emtansine show enhanced clinical responses compared to those treated with lapatinib and capecitabine.[34]

While antibody-drug conjugate therapies show good clinical responses, they do not protect their drug payload during circulation, they typically carry only two to four drug molecules per antibody, and they have no ability to control the drug release kinetics.[35] Nanoparticles carrying anticancer drugs with antibodies on their surfaces can be used to protect and increase the payload of the anticancer drugs. Additionally, drug release kinetics from the nanoparticles can be tuned to provide a variety of behaviors. For instance, drugs (like CPT) that interact with integral components of the cell cycle are best released over long periods of time. This is to allow for long-term, effective intracellular drug concentrations since only a fraction of the cells are cycling at any given time.

Recently, antibody targeted nanoparticle delivery systems are increasingly being investigated.[36–39] In these formulations, there are many antibody molecules contained on the surface of the nanoparticles. One question that has not yet been addressed is whether a single-antibody molecule that is contained on the surface of the nanoparticle can affect the properties of the nanoparticle. In other words, can a nanoparticle that contains one antibody (a more close analogy to an antibody-drug conjugate) show functions of both the single antibody and the nanoparticle? Additionally, can a single-antibody placed on a nanoparticle containing anticancer drugs enhance its antitumor efficacy over the drug containing nanoparticle analog? These are the questions that we begin to address here.

We have recently created a targeted nanoparticle delivery system for CPT through the application of boronic acid-diol complexation.[40] Hydrophobic CPT conjugated onto a biocompatible hydrophilic copolymer of mucic acid and polyethylene glycol (MAP) self-assembles into MAP-CPT nanoparticles. The antibody Herceptin is attached to the MAP-CPT nanoparticle by the use of a boronic acid (via a polyethylene glycol (PEG) spacer). This boronic acid-containing targeting moiety is then complexed with the diol-containing MAP to form a targeted MAP-CPT nanoparticle (Scheme 1). We have shown that targeting of MAP-CPT nanoparticles via a single Herceptin antibody is capable of achieving receptor mediated uptake in BT-474 cells, a HER2 overexpressing human breast cancer cell line *in vitro*.[40] To date, no single-antibody targeted nanoparticle (that is, one antibody molecule per nanoparticle) carrying anticancer drugs has been investigated *in vivo*. We therefore examined the antitumor efficacies of nanoparticles that have on average a single antibody versus nontargeted MAP-CPT nanoparticles in a mouse xenograft model to determine whether a single-antibody on a nanoparticle can provide targeting *in vivo*.

Experimental Section

Materials

Breast carcinoma cell line BT-474 was purchased from American Type Culture Collection (Manassas, VA). Cells were maintained in RPMI-1640 medium supplemented with 10% fetal calf serum (Cellgro, Manassas, VA). Female BALB/c and NCr nude mice were purchased from Jackson Laboratory (Bar Harbor, ME) and Taconic (Oxnard, CA) respectively. 17β-estradiol pellets (0.72 mg, 90 day release) were purchased from Innovative Research of America (Sarasota, FL). Herceptin® was obtained from Dr. Y. Yen at the City of Hope (Duarte, CA). Campthothecin was purchased from Boehringer Ingelheim (Ingelheim, Germany). Goat serum was obtained from Vector Laboratories (Burlingame, CA). Rat anti-PEG primary antibody was purchased from AbCam (Cambridge, MA). Alexa Fluor 488 goat anti-rat IgM secondary antibody, Alexa Fluor 633 goat anti-human IgG secondary antibody and Prolong Gold Antifade reagent were obtained from Invitrogen (Grand Island, NY). All other reagents were purchased from Sigma (St Louis, MO) unless otherwise stated.

Medium MAP and nitroPBA-PEG (3-amide-PEG(5kDa), 5-nitrophenylboronic acid) polymers; short, medium and long MAP-CPT nanoparticles; and Herceptin targeted MAP-CPT nanoparticles were synthesized as previously described.[40] Properties of polymers, polymer-drug conjugates and nanoparticles used in this study are listed in Table 1.

HPLC Quantification of CPT

CPT concentrations were analyzed on a HPLC system (Agilent) equipped with a fluorescence detector (excitation 370 nm, emission 440 nm) and a reverse phase column (Synergi 4 μm Hydro-RP 80 Å, Phenomenex) complete with guard column. 50%

acetonitrile, 50% potassium phosphate buffer (10 mM, pH 4) was used as the eluent at a flow rate of 0.5 mL/min.

Animal Care

All animals were treated as per the National Institute of Health Guidelines for Animal Care, and approved by the California Institute of Technology Institutional Animal Care and Use Committee.

Pharmacokinetics

The nanoparticles formulated in 0.9 wt% NaCl (nontargeted nanoparticles) or PBS (Herceptin targeted MAP-CPT nanoparticles) were administered via bolus, tail vein injection into 12–16 week old female BALB/c mice. At predetermined time points, blood was collected via saphenous vein bleed from individual mice with blood collection tubes (Microvette CB 300 EDTA, Sarstedt). Samples were immediately centrifuged at 10,000 g, 4 °C for 15 min and supernatant was removed and stored at −80 °C until time for analysis. Analyses for unconjugated and polymer-bound CPT were as follows. The amount of unconjugated CPT was determined by first mixing 10 μl of sample with 10 μl of 0.1 N HCl and incubating at room temperature for 30 min. 80 μl of methanol was then added and the mixture incubated at room temperature for 3 h for protein precipitation. This mixture was centrifuged at 14,000 g for 10 min at 4 °C, supernatant was filtered with a 0.45 μm filter (Millex-LH), diluted 20 folds with methanol and 10 μl of the resulting solution was injected into HPLC. The peak area of the eluted CPT (at 7.8 min) was compared to that of control (known concentrations of CPT). To measure the total amount of CPT, 10 μl of sample was mixed with 6.5 μl of 0.1 N NaOH. This solution was incubated at room temperature for 1 h for CPT to be released from parent polymer. 10 μl of 0.1 N HCl was then added to convert the carboxylate CPT form to the lactone form. 73.5 μl of methanol was subsequently added and mixture incubated for 3 h at room temperature. The sample was then centrifuged and processed as above. Polymer-bound CPT concentration was determined from the difference between total CPT and unconjugated CPT concentrations. Non-compartmental modeling software, PK Solutions 2.0 by Summit Research Services (Montrose, CO), was used for pharmacokinetic data analysis.

Maximum Tolerable Dose (MTD)

12 week old female NCr nude mice were randomly divided into thirteen groups containing five mice each. Medium MAP and nitroPBA-PEG polymers at 200 mg/kg; short MAP-CPT nanoparticles at 10, 15 and 20 mg/kg (CPT basis); medium MAP-CPT nanoparticles at 8, 10 and 15 mg/kg (CPT basis); long MAP-CPT nanoparticles at 5, 8 and 10 mg/kg (CPT basis) and the Herceptin targeted MAP-CPT nanoparticles at 8 and 10 mg/kg (CPT basis) were administered on day 0 and day 7 via intravenous tail vein injections. All injections were formulated in 0.9 w/v% saline except for the Herceptin targeted MAP-CPT nanoparticles that were formulated in PBS, pH 7.4. Weight and health of the mice were recorded and monitored daily for 2 weeks after the start of the treatment. MTD was defined as the highest dose resulting in less than 15% body weight loss and with no treatment-related deaths. Animals were euthanized when the criteria for the MTD was exceeded, or at the end of the study by CO_2 asphyxiation.

Biodistribution

7 week old NCr nude mice were transplanted subcutaneously with 17β-estradiol pellets. After 2 days, BT-474 carcinoma cells suspended in RPMI-1640 medium were injected subcutaneously into the front flank at 10 million cells/animal. Treatment began a day after the tumors reached an average size of 260 mm^3 (after 5 days). Animals were randomized

into two groups of six mice per group and were treated via intravenous tail vein injections with either MAP-CPT nanoparticles at 5 mg CPT/kg or Herceptin targeted MAP-CPT nanoparticles at 5 mg CPT/kg and 29 mg Herceptin equivalent/kg (all formulated in PBS, pH 7.4). After 4 h and 24 h, blood was collected from three animals from each group via saphenous vein bleed. These animals were then euthanized by CO_2 asphyxiation and perfused with PBS. Tumor, lung, heart, spleen, kidney and liver were harvested and sectioned into two approximately equal sized pieces. One piece was embedded in Tissue-Tek® OCT (Sakura) and the other was collected in an Eppendorf tube. Samples were frozen immediately at −80 °C until time for processing.

Organs were weighed and 100 mg of each were placed in Lysing Matrix A homogenizer tubes containing an added ¼ inch ceramic spheres (MP Biomedicals, Solon, Ohio). 1 mL of RIPA lysis buffer (Thermo Scientific) was added and tissues were homogenized using a FastPrep®-24 homogenizer (MP Biomedicals, Solon, Ohio) at 6 m/s for 30 s. This was repeated for 3 times with 1 min of cooling on ice in between each round. Samples were centrifuged at 14,000 g for 15 min at 4 °C and supernatants were collected. The amount of unconjugated CPT was determined by first mixing 10 μl of the supernatant with 10 μl of 0.1 N HCl and incubating at room temperature for 30 min. 80 μl of methanol was then added and the mixture incubated at room temperature for 3 h for protein precipitation. This mixture was centrifuged at 14,000 g for 10 min at 4 °C. Supernatant was filtered with a 0.45 μm filter (Millex-LH) and 10 μl of the resulting mixture was injected into HPLC. The peak area of the eluted CPT (at 7.8 min) was compared to that of control (known concentrations of CPT). To measure the total amount of CPT, 10 μl of sample was mixed with 6.5 μl of 0.1 N NaOH. This solution was incubated at room temperature for 1 h for CPT to be released from its parent polymer. 10 μl of 0.1 N HCl was then mixed in to convert carboxylate CPT form to lactone form. 73.5 μl of methanol was subsequently added and the mixture was incubated for 3 h at room temperature. The sample was then centrifuged and processed as above.

Tumor Processing and Confocal Imaging

Tumors were sectioned using a cryostat into a thickness of 20–30 μm. The tumor sections were placed on Superfrost Plus slides (Fisher Scientific, Hampton, NH) and stored at −80 °C until time for further processing. Slides were defrosted and tissue sections were fixed onto the slide for 15 min with a 10% formalin solution. The slides were washed with PBS and blocked for 1 h in a 5% goat serum blocking buffer. A rat anti-PEG primary antibody (14 μg/mL) that recognizes the internal PEG units was placed on the slides and the slides were incubated at 4 °C overnight. They were then washed with PBS and incubated for 1 h with Alexa Fluor 488 goat anti-rat IgM secondary antibody (2 μg/mL). The slides were washed with PBS and incubated for 1 h with Alexa Fluor 633 goat anti-human IgG secondary antibody (2 μg/mL) to visualize Herceptin. They were washed one last time with PBS, mounted with a Prolong Gold Antifade reagent and stored at 4 °C until time for imaging.

Images were acquired with a Zeiss LSM 510 Meta Confocal Microscope (Carl Zeiss, Germany) using a 63× Plan-Neofluar oil objective. 2-Photon excitation at 720 nm (emission filter BP 390–465 nm) was used to detect CPT. Excitation at 488 nm (emission filter LP 530) and at 633 nm (emission filter BP 645–700 nm) were used to detect PEG and Herceptin respectively. All laser and gain settings were set at the beginning of the imaging and were unchanged. Image analysis was performed with a Zeiss LSM image browser.

Antitumor Efficacy Studies

17β-estradiol pellets were transplanted subcutaneously into 7 week old NCr nude mice. After 2 days, BT-474 human breast cancer cells suspended in RPMI-1640 medium were injected subcutaneously into the front flank at 10 million cells/animal. Treatment began a

day after tumors reached an average size of 250 mm^3 (after 5 days). Animals were randomized into nine groups of six to eight mice per group. MAP-CPT nanoparticles at 1 mg and 8 mg/kg (CPT basis, in PBS, pH 7.4), CPT at 8 mg/kg (in 20% DMSO, 20% PEG 400, 30% ethanol and 30% 10 mM pH 3.5 phosphoric acid), Irinotecan at 80 mg/kg (in 5 w/v% dextrose solution, D5W), saline, Herceptin at 2.9 and 5.9 mg/kg (in PBS, pH 7.4), Herceptin targeted MAP-CPT nanoparticles at 0.5 mg CPT/kg and 2.9 mg Herceptin equivalent/kg, and 1 mg CPT/kg and 5.9 mg Herceptin equivalent/kg (in PBS, pH 7.4) were freshly prepared and given via intravenous tail vein injections. Injections were standardized at 150 μl per 20 g body weight of mice. Treatments containing Herceptin were given once per week for 2 weeks. All other groups were given once per week for 3 weeks. Tumor sizes were recorded thrice a week using caliper measurements (length × $width^2/2$) and health of the animals was continuously monitored. Animals were euthanized when tumor volumes exceeded 1000 mm^3. Six weeks after beginning of the treatment, all animals were euthanized by CO_2 asphyxiation.

When animals exited the study due to either tumor size exceeding animal protocol care limits, or treatment-related or non-treatment-related deaths, the last tumor volume value recorded was included in the subsequent data points presented. Two-tailed statistical analyses were conducted at $P = 0.05$. Results were considered significant at $0.01 \leq P \leq 0.05$ and highly significant at $P < 0.01$.

Results and Discussion

Pharmacokinetics

Plasma pharmacokinetic studies of short, medium, long MAP-CPT nanoparticles and Herceptin targeted MAP-CPT nanoparticles at 10 mg/kg (CPT basis) injections were conducted in female BALB/c mice (Fig. 1). Non-compartmental modeling was used for data analysis (Table 2).

Plasma pharmacokinetics of the polymer-bound CPT for all nanoparticle formulations displayed biphasic profiles with fast redistribution phases (α) and long elimination phases (β) (Fig. 1A). The elimination phases for the medium and long MAP-CPT nanoparticles were particularly prolonged with half-lives of 16.6 and 17.6 h, respectively, and showed high AUC values of 2298 and 3636 μg.h/mL, respectively (Table 2). 24 h after injection, 11.3% of the injected dose of the medium MAP-CPT nanoparticles and 20.5% of the injected dose of the long MAP-CPT nanoparticles were still circulating in plasma as polymer-bound CPT (Fig. 1A). In addition, they exhibited small volumes of distribution and low clearance rates. In contrast, male (BALB/c × DBA/2)F_1 mice injected with CPT alone at 10 mg/kg showed fast clearance, with an AUC of only 1.6 μg.h/mL (Table 2, modified from reference 41). Herceptin on the medium MAP-CPT nanoparticles affected their pharmacokinetic profile by increasing the redistribution phase and prolonging the elimination phase to 21.2 h with a high AUC value of 2766 μg.h/mL. The amounts of unbound CPT in plasma for all nanoparticle formulations were low at all time points (Fig. 1B).

Maximum Tolerable Dose (MTD)

MTD values were defined as the highest dose resulting in less than 15% body weight loss with no treatment-related deaths. Female NCr nude mice treated with medium MAP, the nitroPBA-PEG polymer, the short, medium and long MAP-CPT nanoparticles, and the Herceptin-containing MAP-CPT nanoparticles were weighed and monitored for health after doses on day 0 and day 7 (Table 3 and Supplementary Fig. 1).

The weight and health of the mice were unaffected by treatment at high doses of medium MAP or nitroPBA-PEG polymers, indicating low toxicities for these polymeric components. For groups containing CPT, maximum weight loss appeared 3 to 5 days after each treatment. The majority of the groups gained back the lost weight. If body weight loss continued and exceeded an average of 15%, then the study was concluded. Some mice in groups treated with the medium MAP-CPT nanoparticles at 15 mg/kg and the long MAP-CPT nanoparticles at 10 mg/kg showed diarrhea and appeared weak. All other mice appeared healthy. MTD values were found to be 20, 10, 8 and 8 mg/kg (on CPT basis) for the short, medium, long MAP-CPT nanoparticles, and the Herceptin-containing MAP-CPT nanoparticles, respectively (Table 3).

Biodistribution

The percentage injected dose (ID) of total CPT per gram of tumor, heart, liver, spleen, kidney and lung is shown in Fig. 2A. 4 h after dosing, 5.3 and 5.2% ID of total CPT were present per gram of tumor in mice treated with MAP-CPT nanoparticles and Herceptin targeted MAP-CPT nanoparticles, respectively. 24 h after treatment, 2.6% ID of total CPT remained per gram of tumor for mice treated with MAP-CPT nanoparticles, while 3.2% ID of total CPT were found per gram of tumor for mice receiving Herceptin targeted MAP-CPT nanoparticles. These data show that targeting does not enhance the localization of nanoparticles into the tumor site, and this result is consistent with literature observations.[15–17] Additionally, similar distributions of CPT in heart, liver, kidney and lung were observed for nontargeted and targeted nanoparticles. There was, however, a significant amount of total CPT accumulation in the spleen for Herceptin targeted MAP-CPT nanoparticles compared to the nontargeted nanoparticles at 24 h. Significant accumulation in the spleen has been observed previously for humanized antibodies in mice.[42] Since the Herceptin targeted nanoparticles show increased accumulation in the spleen compared to that of the nontargeted nanoparticles, this result implies that during the biodistribution of the Herceptin targeted nanoparticles, the Herceptin is remaining associated with the nanoparticle.

Figure 2B shows the percentage of total CPT in each organ that is present in its unconjugated form. The percentage of unconjugated CPT in heart, liver, spleen, kidney and lung were low at both 4 h and 24 h. In the tumor at 24 h, there were significantly higher percentages of unconjugated CPT for both MAP-CPT nanoparticles and Herceptin targeted MAP-CPT nanoparticles compared to that at 4 h. The retention of unconjugated CPT within the tumors suggests cellular accumulation of CPT. The Herceptin targeted nanoparticles shows slightly higher percentage of unconjugated CPT in tumors compared to the nontargeted nanoparticles at both 4 and 24 h.

The total concentration of CPT in plasma and the percentage of total CPT in plasma that is present in its unconjugated form were similar for both MAP-CPT nanoparticles and Herceptin targeted MAP-CPT nanoparticles (Fig. 2C). After 4 h, 17 and 20 μg/mL of total CPT remained in plasma for MAP-CPT nanoparticles and Herceptin targeted MAP-CPT nanoparticles, respectively. After 24 h, the amounts of total CPT remaining in plasma were the same for both the MAP-CPT nanoparticles and Herceptin targeted MAP-CPT nanoparticles (12 μg/mL). The percentages of total CPT in plasma that were unconjugated to the polymer were below 3% for all conditions indicating fast clearance of unconjugated CPT from plasma (Fig. 2D).

Confocal Imaging of Tumor Tissues

BT-474 tumor bearing NCr nude mice were treated with either MAP-CPT nanoparticles (5 mg CPT/kg) or the Herceptin targeted MAP-CPT nanoparticles (5 mg CPT/kg, 29 mg

Herceptin equivalent/kg). After 4 and 24 h, mice were euthanized and tumors were removed and processed for confocal, immunofluorescence imaging. CPT is intrinsically fluorescent with excitation at 370 nm and emission at 440 nm. To identify the location of the MAP, the PEG component within the MAP was first stained with an anti-PEG antibody; it was then stained with a secondary antibody containing Alexa Fluor 488 (emission 519 nm). All tumor sections were also stained for Herceptin with an anti-human IgG labeled with Alexa Fluor 633 (emission 647 nm). Images of the tumor section were taken at the same laser power and gain settings. Representative images for each group are illustrated in Fig. 3.

Figure 3A shows tumor section of mice treated with MAP-CPT nanoparticles after 4 h. CPT signal was disperse, and signals for CPT and MAP appeared to colocalize in the merged image. 24 h after injection, there was accumulation of CPT signal in the form of punctate spots, and the merged image suggests colocalization of CPT and MAP (Fig. 3B). For mice treated with Herceptin targeted MAP-CPT nanoparticles, spots indicating CPT accumulation were observed after both 4 and 24 h of treatment (Figs. 3C and 3D). In addition, there were colocalizations of the CPT and the MAP signals in the merged images. The presence of Herceptin in the Herceptin targeted MAP-CPT nanoparticles sample is indicated by the strong blue signals in the Herceptin channel compared to the weak background signals in the nontargeted version.

Antitumor Efficacy Studies

One of the most resistant breast cancer cell lines to anticancer drugs (including CPT) is BT-474.[43] We therefore chose this aggressive cell line to generate a tumor model to evaluate the efficacy of our system. To promote tumor growth in nude mice, 17β-estradiol pellets were implanted two days prior to BT-474 tumor cell implantation. On day 0 (5 days after cell implantation), tumor sizes reached an average of 250 mm^3. Treatments via intravenous tail vein injections began on day 1. Irinotecan was administered at a dose of 80 mg/kg in 5 w/v% dextrose solution (D5W). CPT is highly insoluble in aqueous solutions, therefore, it was dissolved in a solution containing 20% DMSO, 20% PEG 400, 30% ethanol and 30% 10 mM pH 3.5 phosphoric acid (a low pH was chosen to retain the CPT in its active lactone form). A saline treatment group was used as the control. All other treatment groups were administered in PBS at pH 7.4. Changes in tumor sizes were recorded by caliper measurement thrice a week and the health of the animals was continuously monitored.

Five weeks after 17β-estradiol pellet implantations, several mice irrespective of treatment groups showed distended bladder and abdominal bloating. This was likely due to the use of 17β-estradiol pellets, which is known to cause hydronephrosis and urine retention in athymic nude mice.[44] Six weeks after treatment, conditions became worse and more mice were observed to develop distended bladders and abdominal bloating. These animals were euthanized.

Tumors in the control group administered with saline grew rapidly (Fig. 4). After 28 days, five out of the eight mice had tumors exceeding the size limit of 1000 mm^3. All animals in this group were euthanized at this time.

Animals treated with CPT (8 mg/kg) resulted in no tumor inhibition compared to that of the control group ($P > 0.05$). One treatment-related death was recorded on day 9, and another three were recorded on day 16. On day 28, four euthanizations were carried out due to tumor sizes exceeding the size limit. None of the animals survived to the end of the study.

Mice treated with Irinotecan at 80 mg/kg showed non-significant tumor inhibition compared to that of the control group ($P > 0.05$). One treatment-related death occurred on day 11. Tumor sizes reached an average of 575 mm^3 by the end of the study.

Animals receiving MAP-CPT nanoparticles at 8 mg CPT/kg showed highly significant tumor inhibition compared to that of the control group ($P < 0.01$). By the end of the study, the mean tumor size was reduced to 63 mm^3 from an initial average volume of 250 mm^3. Three out of the eight mice treated had complete tumor regression. Although no deaths occurred in the MTD study using non-tumor bearing NCr nude mice treated with the MAP-CPT nanoparticles at 8 mg CPT/kg, one death occurred in this study due to weight loss on day 21. This death could be due to the effects of the added tumor burden and/or because mice used in this study were 7 weeks old, while in the MTD studies, 12 week old mice were used.

Animals treated with Herceptin at 5.9 mg/kg showed highly significant tumor inhibition compared to that of the control group ($P < 0.01$). On day 11 of the treatment, seven out of the eight animals treated showed significant tumor regression. However, by the end of the study, two of the regressed tumors relapsed, resulting in a total of five animals with tumors at zero volumes and a group mean tumor volume of 60 mm^3 (Individual animal tumor data are shown in Supplementary Fig. 2A).

The group treated with the MAP-CPT nanoparticles at 1 mg CPT/kg was terminated early due to no observed antitumor effects.

When Herceptin at a dose equivalent of 5.9 mg/kg was added as a targeting agent via a nitroPBA-PEG linker onto the MAP-CPT nanoparticles with a low CPT dose of 1 mg/kg (Herceptin targeted MAP-CPT nanoparticles at 5.9 mg Herceptin equivalent/kg and 1 mg CPT/kg), all tumors regressed to zero on day 9 of treatment and remained at zero by the end of the study (individual animal tumor data are shown in Supplementary Fig. 2B). This result is highly significant compared to that of the control group ($P < 0.01$). One non-treatment-related death occurred on day 37. The combination of antitumor results observed for the Herceptin at 5.9 mg/kg, the MAP-CPT nanoparticles at 1 mg CPT/kg and the Herceptin targeted MAP-CPT nanoparticles (at 5.9 mg Herceptin equivalent/kg and 1 mg CPT/kg) indicate that there is improved antitumor efficacy of the MAP-CPT nanoparticles due to the incorporation of on average a single Herceptin targeting agent.

Animals treated with Herceptin at 2.9 mg/kg resulted in two animals having tumors regressed to zero by the end of the study. The average tumor size increased from the beginning of the study at 250 mm^3 to 278 mm^3 by the end of the study. This result is significant compared to that of the control group ($0.01 \leq P \leq 0.05$).

When animals were treated with the Herceptin targeted MAP-CPT nanoparticles containing 0.5 mg CPT/kg and 2.9 mg Herceptin equivalent/kg, two tumors regressed to zero. The average tumor size was reduced to 141 mm^3 by the end of the study. This result is highly significant compared to that of the control group ($P < 0.01$). The antitumor results from animals treated with Herceptin at 2.9 mg/kg and the Herceptin targeted MAP-CPT nanoparticles (at 2.9 mg Herceptin equivalent/kg and 0.5 mg CPT/kg) further indicate the effectiveness of a nanoparticle that contains on average a single Herceptin.

Summary

Here, we report the *in vivo* behavior of a single-antibody targeted nanoparticle delivery system. The targeted delivery of camptothecin (CPT) conjugated onto a mucic acid containing polymer (MAP) was achieved by using a boronic acid-diol complexation methodology with on average one Herceptin antibody per nanoparticle as the targeting agent.[40] Pharmacokinetics of both MAP-CPT nanoparticles and Herceptin targeted MAP-CPT nanoparticles demonstrated prolonged circulation *in vivo*. Both nontargeted and targeted nanoparticles showed similar biodistributions, except for increased accumulation of

the targeted nanoparticle in the spleen that can be attributed to the antibody remaining associated with the nanoparticle during its biodistributon. In mice bearing HER2 overexpressing BT-474 human breast cancer tumors, the effect of on average one Herceptin antibody per MAP-CPT nanoparticle was sufficient to result in complete tumor regression, as well as superior antitumor activity compared to that of the nontargeted MAP-CPT nanoparticles and the Herceptin antibody alone groups. The roles of the antibody on the nanoparticle were to alter the behavior of the nanoparticle within the solid tumor (Herceptin can enhance BT-474 cell uptake) and to provide a therapeutic effect (Herceptin is active in BT-474 cells).

Supplementary Material

Refer to Web version on PubMed Central for supplementary material.

Acknowledgments

We thank Leonard Medrano, Aaron Gale and Devin Wiley for assistance with animal work, tumor processing and confocal microscopy, respectively. This project was financially supported by the National Cancer Institute Grant CA 151819.

References

(1). Hsiang YH, Hertzberg R, Hecht S, Liu LF. Camptothecin Induces Protein-Linked DNA Breaks Via Mammalian DNA Topoisomerase-I. J. Biol. Chem. 1985; 260:4873–4878.

(2). Rapisarda A, Uranchimeg B, Scudiero DA, Selby M, Sausville EA, Shoemaker RH, Melillo G. Identification of small molecule inhibitors of hypoxia-inducible factor 1 transcriptional activation pathway. Cancer Res. 2002; 62:4316–4324. [PubMed: 12154035]

(3). Moertel CG, Schutt AJ, Reitemeier RJ, Hahn RG. Phase II study of camptothecin (NSC-100880) in the treatment of advanced gastrointestinal cancer. Cancer Chemother Rep. 1972; 56:95–101. [PubMed: 5030811]

(4). Muggia FM, Selawry OS, Hansen HH, Creaven PJ, Cohen MH. Phase I clinical trial of weekly and daily treatment with camptothecin (NSC-100880): correlation with preclinical studies. Cancer Chemother. Rep. 1972; 56:515–521. [PubMed: 5081595]

(5). Mi ZH, Burke TG. Marked Interspecies Variations Concerning the Interactions of Camptothecin with Serum Albumins - a Frequency-Domain Fluorescence Spectroscopic Study. Biochemistry. 1994; 33:12540–12545. [PubMed: 7918477]

(6). Xu Y, Villalona-Calero MA. Irinotecan: mechanisms of tumor resistance and novel strategies for modulating its activity. Ann. Oncol. 2002; 13:1841–1851. [PubMed: 12453851]

(7). Mathijssen RHJ, van Alphen RJ, Verweij J, Loos WJ, Nooter K, Stoter G, Sparreboom A. Clinical pharmacokinetics and metabolism of irinotecan (CPT-11). Clin. Cancer Res. 2001; 7(8):2182–2194. [PubMed: 11489791]

(8). Ando Y, Saka H, Ando M, Sawa T, Muro K, Ueoka H, Yokoyama A, Saitoh S, Shimokata K, Hasegawa Y. Polymorphisms of UDP-glucuronosyltransferase gene and irinotecan toxicity: A pharmacogenetic analysis. Cancer Res. 2000; 60:6921–6926. [PubMed: 11156391]

(9). Tian Q, Zhang J, Chan SY, Tan TMC, Duan W, Huang M, Zhu YZ, Chan E, Yu Q, Nie YQ, Ho PCL, Li Q, Ng KY, Yang HY, Wei H, Bian JS, Zhou SF. Topotecan is a substrate for multidrug resistance associated protein 4. Curr. Drug Metab. 2006; 7:105–116. [PubMed: 16454695]

(10). Svenson S, Wolfgang M, Hwang J, Ryan J, Eliasof S. Preclinical to clinical development of the novel camptothecin nanopharmaceutical CRLX101. J. Control. Release. 2011; 153:49–55. [PubMed: 21406204]

(11). Homsi J, Simon GR, Garrett CR, Springett G, De Conti R, Chiappori A, Munster PN, Burton MK, Stromatt S, Allievi C, Angiulli P, Eisenfeld A, Sullivan DM, Daud AI. Phase I trial of poly-L-glutamate camptothecin (CT-2106) administered weekly in patients with advanced solid malignancies. Clin. Cancer Res. 2007; 13:5855–5861. [PubMed: 17908979]

(12). Yurkovetskiy AV, Fram RJ. XMT-1001, a novel polymeric camptothecin pro-drug in clinical development for patients with advanced cancer. Adv. Drug Deliver. Rev. 2009; 61:1193–1202.

(13). Scott L, Yao J, Benson AB, Thomas A, Falk S, Mena R, Picus J, Wright J, Mulcahy M, Ajani J, Evans T. A phase II study of pegylated-camptothecin (pegamotecan) in the treatment of locally advanced and metastatic gastric and gastro-oesophageal junction adenocarcinoma. Cancer Chemother. Pharm. 2009; 63:363–370.

(14). Maeda H, Wu J, Sawa T, Matsumura Y, Hori K. Tumor vascular permeability and the EPR effect in macromolecular therapeutics: a review. J. Control. Release. 2000; 65:271–284. [PubMed: 10699287]

(15). Kirpotin DB, Drummond DC, Shao Y, Shalaby MR, Hong KL, Nielsen UB, Marks JD, Benz CC, Park JW. Antibody targeting of long-circulating lipidic nanoparticles does not increase tumor localization but does increase internalization in animal models. Cancer Res. 2006; 66:6732–6740. [PubMed: 16818648]

(16). Bartlett DW, Su H, Hildebrandt IJ, Weber WA, Davis ME. Impact of tumor-specific targeting on the biodistribution and efficacy of siRNA nanoparticles measured by multimodality in vivo imaging. Proc. Natl. Acad. Sci. U.S.A. 2007; 104:15549–15554. [PubMed: 17875985]

(17). Choi CHJ, Alabi CA, Webster P, Davis ME. Mechanism of active targeting in solid tumors with transferrin-containing gold nanoparticles. Proc. Natl. Acad. Sci. U.S.A. 2010; 107:1235–1240. [PubMed: 20080552]

(18). Scott AM, Wolchok JD, Old LJ. Antibody therapy of cancer. Nat. Rev. Cancer. 2012; 12:278–287. [PubMed: 22437872]

(19). Janthur WD, Cantoni N, Mamot C. Drug Conjugates Such as Antibody Drug Conjugates (ADCs), Immunotoxins and Immunoliposomes Challenge Daily Clinical Practice. Int. J. Mol. Sci. 2012; 13:16020–16045. [PubMed: 23443108]

(20). Luedke E, Jaime-Ramirez AC, Bhave N, Carson WE. Monoclonal Antibody Therapy of Pancreatic Cancer With Cetuximab: Potential for Immune Modulation. J. Immunother. 2012; 35:367–373. [PubMed: 22576341]

(21). Slamon DJ, Clark GM, Wong SG, Levin WJ, Ullrich A, Mcguire WL. Human-Breast Cancer - Correlation of Relapse and Survival with Amplification of the Her-2 Neu Oncogene. Science. 1987; 235:177–182. [PubMed: 3798106]

(22). Slamon DJ, Godolphin W, Jones LA, Holt JA, Wong SG, Keith DE, Levin WJ, Stuart SG, Udove J, Ullrich A, Press MF. Studies of the Her-2/Neu Proto-Oncogene in Human-Breast and Ovarian-Cancer. Science. 1989; 244:707–712. [PubMed: 2470152]

(23). Slamon DJ, Leyland-Jones B, Shak S, Fuchs H, Paton V, Bajamonde A, Fleming T, Eiermann W, Wolter J, Pegram M, Baselga J, Norton L. Use of chemotherapy plus a monoclonal antibody against HER2 for metastatic breast cancer that overexpresses HER2. New Engl. J. Med. 2001; 344:783–792. [PubMed: 11248153]

(24). Smith I, Procter M, D Gelber R, Guillaume S, Feyereislova A, Dowsett M, Goldhirsch A, Untch M, Mariani G, Baselga J, Kaufmann M, Cameron D, Bell R, Bergh J, Coleman R, Wardley A, Harbeck N, Lopez RI, Mallmann P, Gelmon K, Wilcken N, Wist E, Rovira PS, Piccart-Gebhart M. 2-year follow-up of trastuzumab after adjuvant chemotherapy in HER2-positive breast cancer: a randomised controlled trial. Lancet. 2007; 369:29–36. [PubMed: 17208639]

(25). Cobleigh MA, Vogel CL, Tripathy D, Robert NJ, Scholl S, Fehrenbacher L, Wolter JM, Paton V, Shak S, Lieberman G, Slamon DJ. Multinational study of the efficacy and safety of humanized anti-HER2 monoclonal antibody in women who have HER2-overexpressing metastatic breast cancer that has progressed after chemotherapy for metastatic disease. J. Clin. Oncol. 1999; 17:2639–2648. [PubMed: 10561337]

(26). Vogel CL, Cobleigh MA, Tripathy D, Gutheil JC, Harris LN, Fehrenbacher L, Slamon DJ, Murphy M, Novotny WF, Burchmore M, Shak S, Stewart SJ, Press M. Efficacy and safety of trastuzumab as a single agent in first-line treatment of HER2-overexpressing metastatic breast cancer. J. Clin. Oncol. 2002; 20:719–726. [PubMed: 11821453]

(27). Casi G, Neri D. Antibody-drug conjugates: Basic concepts, examples and future perspectives. J. Control. Release. 2012; 161:422–428. [PubMed: 22306430]

(28). Adair JR, Howard PW, Hartley JA, Williams DG, Chester KA. Antibody-drug conjugates - a perfect synergy. Expert Opin. Biol. Ther. 2012; 12:1191–1206. [PubMed: 22650648]

(29). Younes A, Yasothan U, Kirkpatrick P. Brentuximab vedotin. Nature Rev. Drug Discov. 2012; 11:19–20. [PubMed: 22212672]

(30). Katz J, Janik JE, Younes A. Brentuximab Vedotin (SGN-35). Clin. Cancer Res. 2011; 17:6428–6436. [PubMed: 22003070]

(31). Younes A, Gopal AK, Smith SE, Ansell SM, Rosenblatt JD, Savage KJ, Ramchandren R, Bartlett NL, Cheson BD, de Vos S, Forero Torres, A. Moskowitz CH, Connors JM, Engert A, Larsen EK, Kennedy DA, Sievers EL, Chen R. Results of a Pivotal Phase II Study of Brentuximab Vedotin for Patients With Relapsed or Refractory Hodgkin's Lymphoma. J. Clin. Oncol. 2012; 30:2183–2189. [PubMed: 22454421]

(32). Pro B, Advani R, Brice P, Bartlett NL, Rosenblatt JD, Illidge T, Matous J, Ramchandren R, Fanale M, Connors JM, Yang Y, Sievers EL, Kennedy DA, Shustov A. Brentuximab Vedotin (SGN-35) in Patients With Relapsed or Refractory Systemic Anaplastic Large-Cell Lymphoma: Results of a Phase II Study. J. Clin. Oncol. 2012; 30:2190–2196. [PubMed: 22614995]

(33). Phillips GDL, Li GM, Dugger DL, Crocker LM, Parsons KL, Mai E, Blattler WA, Lambert JM, Chari RVJ, Lutz RJ, Wong WLT, Jacobson FS, Koeppen H, Schwall RH, Kenkare-Mitra SR, Spencer SD, Sliwkowski MX. Targeting HER2-Positive Breast Cancer with Trastuzumab-DM1, an Antibody-Cytotoxic Drug Conjugate. Cancer Res. 2008; 68:9280–9290. [PubMed: 19010901]

(34). Verma S, Miles D, Gianni L, Krop IE, Welslau M, Baselga J, Pegram M, Oh DY, Dieras V, Guardino E, Fang L, Lu MW, Olsen S, Blackwell K. Trastuzumab emtansine for HER2-positive advanced breast cancer. New Eng. J. Med. 2012; 367:1783–91. [PubMed: 23020162]

(35). Hamblett KJ, Senter PD, Chace DF, Sun MMC, Lenox J, Cerveny CG, Kissler KM, Bernhardt SX, Kopcha AK, Zabinski RF, Meyer DL, Francisco JA. Effects of drug loading on the antitumor activity of a monoclonal antibody drug conjugate. Clin. Cancer Res. 2004; 10:7063–7070. [PubMed: 15501986]

(36). Drummond DC, Noble CO, Guo Z, Hayes ME, Connolly-Ingram C, Gabriel BS, Hann B, Liu B, Park JW, Hong K, Benz CC, Marks JD, Kirpotin DB. Development of a highly stable and targetable nanoliposomal formulation of topotecan. J. Control. Release. 2010; 141:13–21. [PubMed: 19686789]

(37). Yang T, Choi MK, Cui FD, Kim JS, Chung SJ, Shim CK, Kim DD. Preparation and evaluation of paclitaxel-loaded PEGylated immunoliposome. J. Control. Release. 2007; 120:169–177. [PubMed: 17586082]

(38). Cirstoiu-Hapca A, Buchegger F, Lange N, Bossy L, Gurny R, Delie F. Benefit of anti-HER2-coated paclitaxel-loaded immuno-nanoparticles in the treatment of disseminated ovarian cancer: Therapeutic efficacy and biodistribution in mice. J. Control. Release. 2010; 144:324–331. [PubMed: 20219607]

(39). Hong MH, Zhu SJ, Jiang YY, Tang GT, Pei YY. Efficient tumor targeting of hydroxycamptothecin loaded PEGylated niosomes modified with transferrin. J. Control. Release. 2009; 133:96–102. [PubMed: 18840485]

(40). Han H, Davis ME. Targeted nanoparticles assembled via complexation of boronic acid-containing targeting moieties to diol-containing polymers. Bioconjugate Chem. 2013; 24:669–677.

(41). Supko JG, Malspeis L. Pharmacokinetics of the 9-Amino and 10,11-Methylenedioxy Derivatives of Camptothecin in Mice. Cancer Res. 1993; 53:3062–3069. [PubMed: 8319213]

(42). Cheng WWK, Allen TM. Targeted delivery of anti-CD19 liposomal doxorubicin in B-cell lymphoma: A comparison of whole monoclonal antibody, Fab' fragments and single chain Fv. J. Control. Release. 2008; 126:50–58. [PubMed: 18068849]

(43). Davis PL, Shaiu WL, Scott GL, Iglehart JD, Hsieh TS, Marks JR. Complex response of breast epithelial cell lines to topoisomerase inhibitors. Anticancer Res. 1998; 18:2919–2932. [PubMed: 9713486]

(44). Gakhar G, Wight Carter M, Andrews G, Olson S, Nguyen TA. Hydronephrosis and urine retention in estrogen-implanted athymic nude mice. Vet. Pathol. 2009; 46:505–8. [PubMed: 19176493]

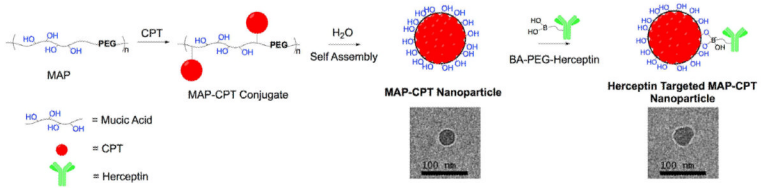

Scheme 1.

Schematic of MAP-CPT nanoparticle and Herceptin targeted MAP-CPT nanoparticle delivery systems. MAP = mucic acid and polyethylene glycol copolymer, CPT = camptothecin, BA = boronic acid. Modified from ref. 40.

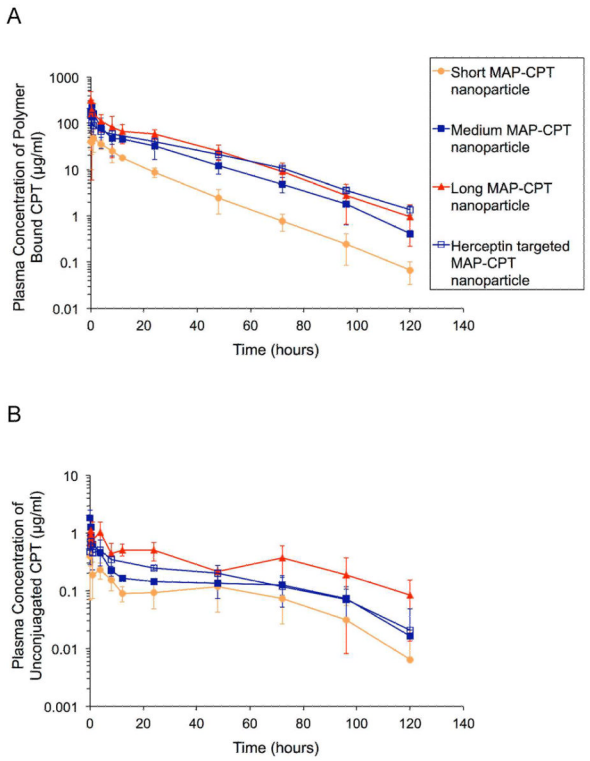

Figure 1.

Plasma pharmacokinetics of short, medium and long MAP-CPT nanoparticles; and Herceptin targeted MAP-CPT nanoparticles in female BALB/c mice at 10 mg CPT/kg injections. (A) Plasma concentration of polymer-bound CPT as a function of time. (B) Plasma concentration of unconjugated CPT as a function of time.

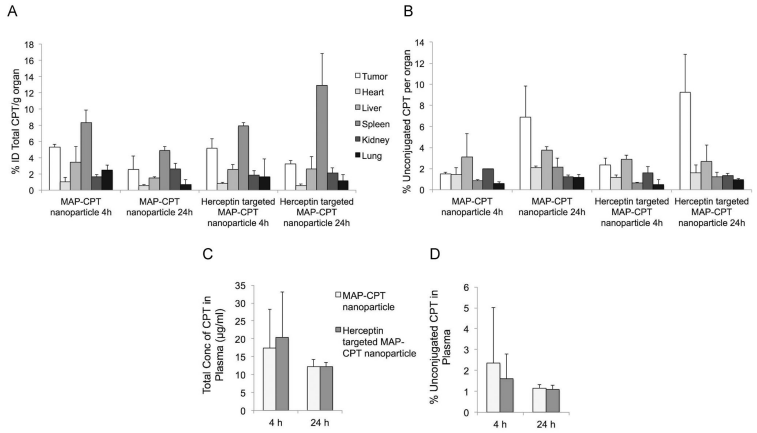

Figure 2.

Biodistribution of MAP-CPT nanoparticles (5 mg CPT/kg) and Herceptin targeted MAP-CPT nanoparticles (5 mg CPT/kg, 29 mg Herceptin equivalent/kg) after 4 and 24 h of treatment in female NCr nude mice bearing BT-474 xenograft tumors. (A) Percent injected dose (ID) of total CPT per gram of tumor, heart, liver, spleen, kidney or lung. (B) Percentage of total CPT in each organ that is unconjugated in tumor, heart, liver, spleen, kidney and lung. (C) Total concentration of CPT in plasma. (D) Percentage of total CPT that is unconjugated in plasma.

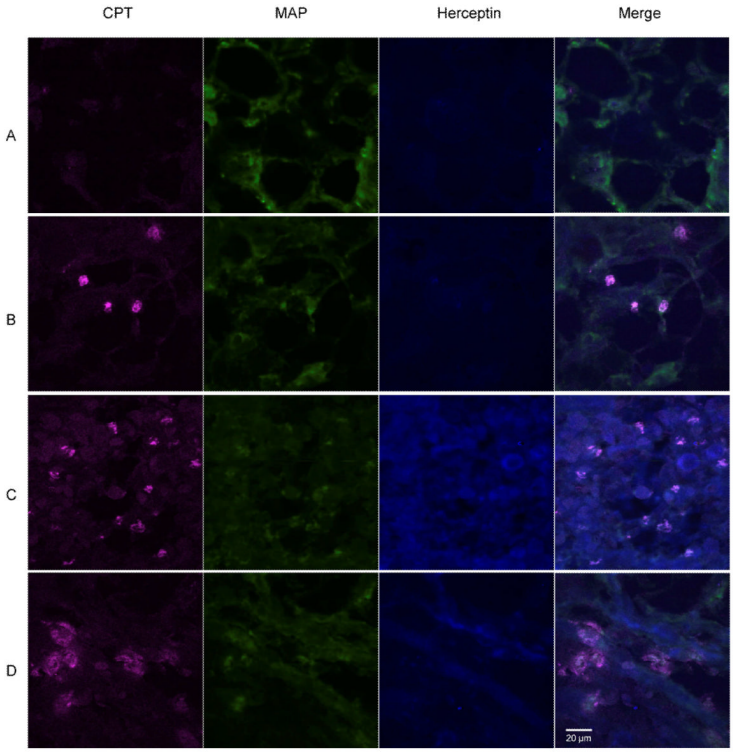

Figure 3.
Confocal immunofluorescence microscopy of BT-474 tumor sections taken from female NCr nude mice treated with (A) MAP-CPT nanoparticles (5 mg CPT/kg) at 4 h (B) MAP-CPT nanoparticles (5 mg CPT/kg) at 24 h. (C) Herceptin targeted MAP-CPT nanoparticles (5 mg CPT/kg, 29 mg Herceptin equivalent/kg) at 4 h. (D) Herceptin targeted MAP-CPT nanoparticles (5 mg CPT/kg, 29 mg Herceptin equivalent/kg) at 24 h. Left panel emission 440 nm (CPT, pink), center left panel emission 519 nm (MAP, green), center right panel emission 647 nm (Herceptin, blue), right panel overlay of images.

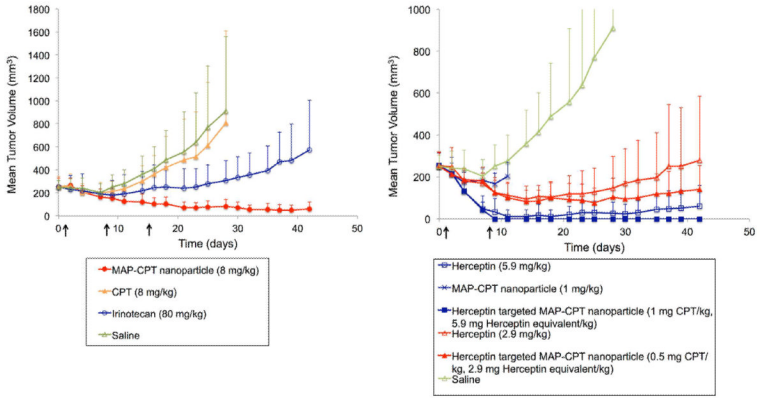

Figure 4.

Antitumor efficacy studies in female NCr nude mice bearing BT-474 xenograft tumors. Mean tumor volumes as functions of time. Groups containing Herceptin received 2 weekly doses, all other groups received 3 weekly doses.

Table 1

Properties of MAP, MAP-CPT conjugate, MAP-CPT nanoparticles and Herceptin targeted MAP-CPT nanoparticles

	MAP	MAP-CPT conjugate	MAP-CPT nanoparticle			Herceptin targeted MAP-CPT nanoparticle		
	MW[a] (kDa)	wt% CPT conjugated	# CPT/particle	particle size (nm)	zeta potential (mV)	# Herceptin/particle	particle size (nm)	zeta potential (mV)
Short	20	9.8	~14	~30	−1.3+/−0.6			
Medium	65	12.7	~60	~30	−0.5+/−0.5	~1	~40	−0.4+/−0.6
Long	102	10.1	~72	~30	−0.8+/−0.5			

[a]MW, molecular weight determined as (Mw+Mn)/2; Mw, weight average molecular weight; Mn, number average molecular weight.

Table 2

Plasma pharmacokinetic parameters of polymer-bound CPT for short, medium and long MAP-CPT nanoparticles; and Herceptin targeted MAP-CPT nanoparticles compared to CPT alone

	$t_{1/2}\alpha$ (h)	$t_{1/2}\beta$ (h)	AUC (μg.h/mL)	Vd (mL)	Cl (mL/h)
Short MAP-CPT nanoparticle	0.6	13.2	728	6.5	0.34
Medium MAP-CPT nanoparticle	1.0	16.6	2298	2.6	0.11
Long MAP-CPT nanoparticle	0.4	17.6	3636	1.7	0.07
Herceptin targeted MAP-CPT nanoparticle	0.2	21.2	2766	2.8	0.09
CPT[41]	-	-	1.6	5538	156

Abbreviations: $t_{1/2}$ α, redistribution half-life; $t_{1/2}$ β, elimination half-life; AUC, area under curve; Vd, volume of distribution; Cl, systemic clearance.

Table 3

Treatment response for maximum tolerable dose (MTD) study

	Dose (mg/kg)[a]	Max % weight loss (day)[b]	Death
Medium MAP	200	−1.1 (11)	0
NitroPBA-PEG polymer	200	−0.5 (2)	0
Short MAP-CPT nanoparticle	10	−4.5 (2)	0
	15	−6.1 (10)	0
	20	−10.2 (12)	0
Medium MAP-CPT nanoparticle	8	−6.8 (10)	0
	10	−14.9 (12)	0
	15	−18.4 (4)	culled[c]
Long MAP-CPT nanoparticle	5	−4.8 (4)	0
	8	−9.2 (12)	0
	10	−16.5 (10)	culled[c]
Herceptin targeted MAP-CPT nanoparticle	8	−5.2 (4)	0
	10	−15.2 (9)	culled[c]

[a] All groups containing MAP-CPT are based on mg CPT/kg.

[b] Maximum percent body weight loss.

[c] Animals culled due to exceeding 15% body weight loss.

Table 4

Antitumor efficacy studies in NCr nude mice bearing BT-474 xenograft tumors

	N_{begin}/N_{end} [a]	$N_{TRD}/N_{NTRD}/N_{euthan}$ [b]	Mean tumor volume (mm^3)	Median tumor volume (mm^3)	$N_{reg\ to\ zero}$ [c]	P vs saline[d]
MAP-CPT nanoparticle (8 mg/kg)	8/7	1/0/0	63	68	3	0.002
Irinotecan (80 mg/kg)	8/7	1/0/0	575	479	0	0.242
CPT (8 mg/kg)	8/0	4/0/4	808	417	0	0.781
Herceptin (5.9 mg/kg)	8/8	0/0/0	60	0	5	0.003
Herceptin targeted MAP-CPT nanoparticle (1 mg CPT/kg, 5.9 mg Herceptin equivalent/kg)	8/7	0/1/0	0	0	7	0.001
Herceptin (2.9 mg/kg)	6/6	0/0/0	278	245	2	0.026
Herceptin targeted MAP-CPT nanoparticle (0.5 mg CPT/kg, 2.9 mg Herceptin equivalent/kg)	6/6	0/0/0	141	187	2	0.005
Saline	8/0	0/0/8	911	1087	0	-

[a] N_{begin} is number of animals at beginning of study, N_{end} is number of animals surviving to end of study.

[b] N_{TRD} is number of treatment-related death, N_{NTRD} is number of non-treatment-related death, N_{euthan} is number of animals euthanized due to exceeding tumor size limit of 1000 mm^3.

[c] $N_{reg\ to\ zero}$ is number of animals with tumors regressed to zero at the end of study.